

Short Communication

## Hierarchically Constructed TiO<sub>2</sub> Spheres as Efficient Polysulfide Barrier for High-Performance Li-S Battery

Luo Jie\*, Zhang Ning

School of Mechanical Engineering, Xijing University, Xi'an, 710123, China.

\*E-mail: [luojixijing@126.com](mailto:luojixijing@126.com)

Received: 22 January 2019 / Accepted: 18 March 2019 / Published: 10 May 2019

Lithium-Sulfur batteries are the most promising candidates for the next energy storage system. Many reports have been reported for improving the cycle performances of Li-S battery, such as designing cathode host material, employing functionalized interlayer between the cathode and separator and developing suitable electrolyte. In this work, novel hierarchically constructed TiO<sub>2</sub> spheres are prepared and used host materials for sulfur cathode. This novel structure of TiO<sub>2</sub> spheres serves as the host material, which could efficiently stabilize the polysulfide at the cathode side. As a result, the shuttle effect of polysulfide in the Li-S battery is greatly alleviated via the hierarchically constructed TiO<sub>2</sub> spheres. Finally, the TiO<sub>2</sub>/S composites display excellent cycle stability and superior rate performance.

**Keywords:** Li-S batteries, Cathode Materials, Electric vehicle, Cycle Stability, TiO<sub>2</sub> Spheres

### 1. INTRODUCTION

With the rapid economic development, environment pollution has become a universal problem all over the world [1, 2]. This is mainly caused by the fossil fuel combustion, which could release toxic gas in the air. Moreover, the large consumption of fossil fuel will lead the energy shortage in the near future [3, 4]. Therefore, it is necessary to search new energy storage system for the researchers [5]. During the past decades, some energy devices have attracted the attention of the scientists who are devote into electrochemical energy storage system, such as Lithium-ion batteries [6, 7], Li-S batteries [8, 9], Li-Air batteries [10]. Among these systems, Li-S batteries are the most promising candidate as the next generation energy storage system, which is due to their advantages of the high specific capacity and energy density [11]. This energy storage system is significant for the electric vehicle. As we all known, the electric vehicle has great demands for the Li-ion batteries and Li-S batteries.

In the past years, many teams and colleges have made efforts on the study of Li-S batteries. The

cycle performance and rate performance are very poor during discharge-charge process at high current densities. This phenomenon is ascribed to the shuttle effect of polysulfide in the electrolyte. Consequently, all works are improving the cycle stability and rate performance of Li-S batteries [12]. Among these works, the most studies focused on the sulfur cathode modification. The cathode materials are the most significant part in the Li-S batteries [13, 14]. Their morphologies and structures have direct effect on the electrochemical performance of the prepared Li-S batteries [15]. Consequently, designing perfect structure for the cathode materials plays an important role in the Li-S batteries.

In this paper, novel hierarchically constructed  $\text{TiO}_2$  spheres are firstly prepared and used host materials for sulfur cathode. This novel structure of  $\text{TiO}_2$  spheres serves as the host material, which could efficiently stabilize the polysulfide at the cathode side. As a result, the shuttle effect of polysulfide in the Li-S battery is greatly alleviated via the hierarchically constructed  $\text{TiO}_2$  spheres. Finally, the  $\text{TiO}_2/\text{S}$  composites display excellent cycle stability and superior rate performance.

## 2. EXPERIMENTAL

### 2.1. Preparation of hierarchically $\text{TiO}_2$ spheres

Firstly, 15 ml titanium isopropoxide (TIP) and 20 ml ethanol were mixed in the beaker. Then, 3 ml  $\text{NH}_3\text{H}_2\text{O}$  was gradually added into the above mixture under stirring. After that, the mixture was kept for 2 h. At last, the sample was washed and dried to obtain hierarchically  $\text{TiO}_2$  spheres. titanium isopropoxide

### 2.2. Preparation of $\text{TiO}_2/\text{S}$ composites

The as-prepared hierarchically  $\text{TiO}_2$  spheres were firstly mixed with sublimed sulfur with a ratio of 1:2. Then, the mixture was transferred into a sealed stainless steel reactor. Finally, the steel reactor was heated at 155 °C for 12 h. After cooling to the room temperature, the sample was grind for 30 min. As a result, the  $\text{TiO}_2/\text{S}$  composites were successfully prepared.

### 2.3. Materials Characterization

The morphologies of the materials were characterized by using scanning electron microscope (SEM, EVO 18) and transmission electron microscope (TEM, Tecnai F20). The diffraction peaks of materials were tested by an X-ray diffractometer (XRD, D8 Advance, BRUKER).

### 2.4. Electrochemical Measurements

The electrochemical performance was measured by using CR 2032 coin-type half cells. First of all, 80 wt.% samples, 10 wt.% super black and 10 wt.% PVDF with NMP were mixed for preparing

slurry. After that, the slurry was uniformly coated on the surface of Al foil. Then, the prepared-film was placed in the vacuum at 80°C for 24 h. Finally, the film was cut into circular electrodes. The cells were assembled in an Ar-filled glove box, lithium foil is anode. The electrolyte was consisted of 1.0 M LiTFSI and EC/DEC. Discharging/charging profiles were carried out on a battery testing system (LandCT2001A) in the voltage between 1.5 V and 3 V.

### 3. RESULTS AND DISCUSSION

To clearly indicate the preparation process of the composites, a diagrammatic sketch was made. As shown in Figure 1, the TiO<sub>2</sub> spheres were firstly prepared via sol-gel method using TIP as the titanium source. After that, the TiO<sub>2</sub> spheres were mixed with elemental sulfur and heated at 155 °C for 12 h. After cooling to the room temperature, the TiO<sub>2</sub>/S composites are successfully prepared. This hierarchically spheres structure could adsorb the S<sub>n</sub><sup>x-</sup>, which is produced during the discharge process of TiO<sub>2</sub>/S composite cathode. Finally, the shuttle effect is efficiently restrained by the novel hierarchically spheres structure.

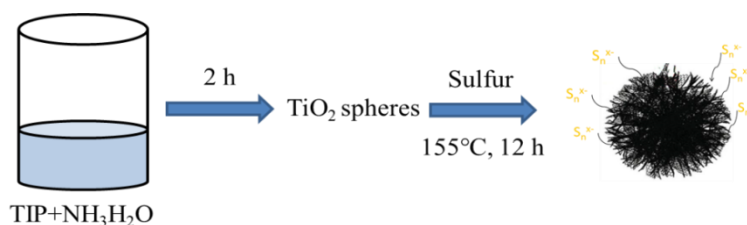


**Figure 1.** The preparation of TiO<sub>2</sub>/S composites by using heating method.

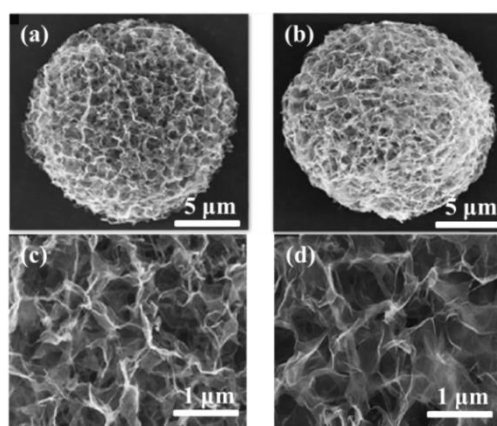


**Figure 2.** (a), (b) The low-magnification SEM of TiO<sub>2</sub> and TiO<sub>2</sub>/S composite. (c), (d) The high-magnification SEM of TiO<sub>2</sub> and TiO<sub>2</sub>/S composite.

To investigate the morphologies of the as-prepared samples, SEM was conducted for the TiO<sub>2</sub> and TiO<sub>2</sub>/S composites. As shown in Figure 2a, the TiO<sub>2</sub> shows hierarchically spheres structure. Its

dimeter is located in the range of 15-20  $\mu\text{m}$ . Figure 2b is the SEM image of  $\text{TiO}_2/\text{S}$  composites. It can be seen that the elemental sulfur is uniformly dispersed in the pores of  $\text{TiO}_2$  spheres. The morphology has no obvious change between  $\text{TiO}_2$  and  $\text{TiO}_2/\text{S}$  composites. Figure 2c and d further display the high-magnification SEM images of  $\text{TiO}_2$  and  $\text{TiO}_2/\text{S}$  composite. As observed from the Figure, the surface of  $\text{TiO}_2$  and  $\text{TiO}_2/\text{S}$  composite is consisted many nano-sheets. These nano-sheets provide adequate active site for the electrochemical reaction during discharge-charge process of  $\text{TiO}_2/\text{S}$  composite cathode in the Li-S batteries.

Figure 3a is the high- magnification TEM image of the  $\text{TiO}_2/\text{S}$  composite. From the Figure 3a, the TEM image indicates the nano-sheet morphology. This is consistent with the SEM results. To confirm the presence of all elements in the  $\text{TiO}_2/\text{S}$  composite, corresponding elemental mapping of  $\text{TiO}_2/\text{S}$  composite was applied. As shown in Figure 3b, c and d, the elements Ti, O and S are uniformly distributed in the whole  $\text{TiO}_2/\text{S}$  composite.

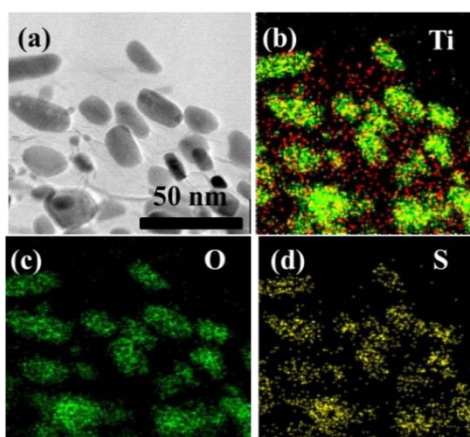


**Figure 3.** (a) The high- magnification TEM image of  $\text{TiO}_2/\text{S}$  composite, corresponding elemental mapping of  $\text{TiO}_2/\text{S}$  composite (b) Ti, (c) O, (d) S.

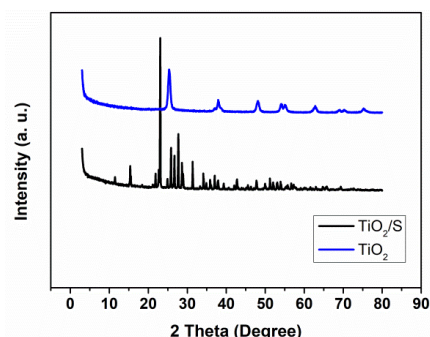
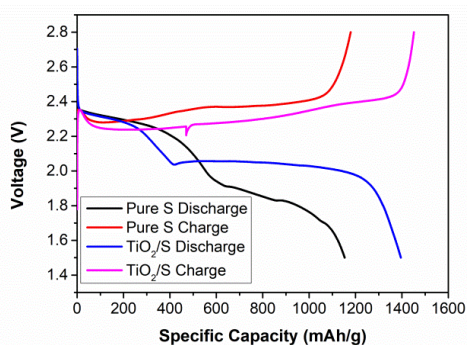


**Figure 4.** The XRD pattern of the  $\text{TiO}_2$  spheres and  $\text{TiO}_2/\text{S}$  composites at 2 theta from  $10^\circ$  to  $80^\circ$ .

The XRD pattern of  $\text{TiO}_2$  and  $\text{TiO}_2/\text{S}$  composites was tested and shown in Figure 4. The  $\text{TiO}_2$  shows typical diffraction peaks at the theta between  $10^\circ$  and  $70^\circ$ . The peak at  $25^\circ$  and  $38^\circ$  represents the crystal plane of (101) and (004), respectively. This result is the same as the works in the reported

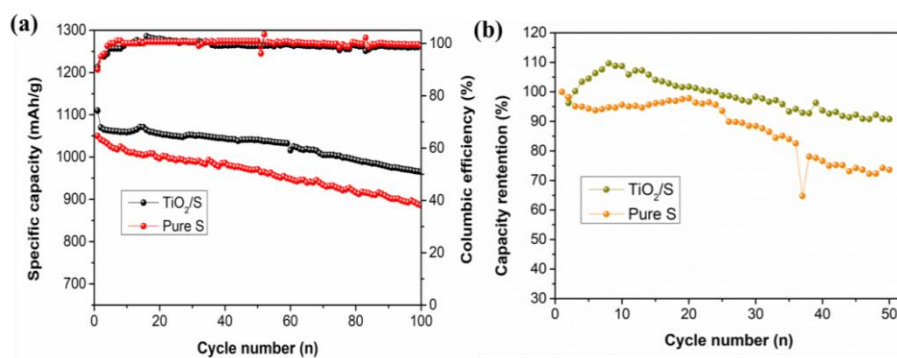
literature [16]. After heated with the sulfur, the peaks of TiO<sub>2</sub>/S composites are similar with the pure sulfur. This is because the diffraction peaks of sulfur are very strong. Therefore, the XRD pattern of TiO<sub>2</sub>/S composite mainly exhibits the peaks of sulfur. In all, these results confirm the successful preparation of TiO<sub>2</sub>/S composite.

The electrochemical performances are the key index for measuring the as-prepared TiO<sub>2</sub>/S composite. The first discharge/charge profiles are tested at the current density of 0.1C. As shown in Figure 5, the profiles of TiO<sub>2</sub>/S and pure S are similar. Both of them have two voltage platforms during the discharge process at 2.3 V and 2.1 V, respectively. Besides, the other information could be obtained from the profiles. The specific capacity value of TiO<sub>2</sub>/S composites is much higher than the pure sulfur. The value of TiO<sub>2</sub>/S composites is 1405 mAh g<sup>-1</sup> at the current density of 0.1 C. This result confirms the positive effect of TiO<sub>2</sub> in the TiO<sub>2</sub>/S composites for improving the specific capacity value of the cathode materials [17, 18].



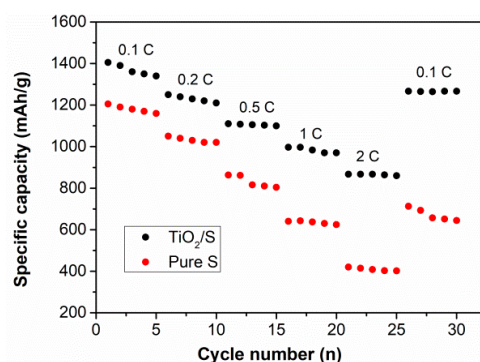
**Figure 5.** The DC curves of pure S and TiO<sub>2</sub>/S composites at the current density of 0.1 C.

Figure 6a shows the cycle stability of two cathode materials at the current density of 0.5 C. The TiO<sub>2</sub>/S composite exhibits capacity value of 1102 mAh g<sup>-1</sup>. After 100 cycles, the capacity value is remained at 968 mAh g<sup>-1</sup>, which demonstrating excellent cycle performance at the high current density. In terms of the pure S cathode, the capacity value is 1051 mAh g<sup>-1</sup> before cycling. This value is only 882 mAh g<sup>-1</sup> after 100 cycles. Even at much higher current density, the TiO<sub>2</sub>/S composite cathode could keep superior cycle stability. As shown in Figure 6b, it exhibits the capacity retention of two cathode materials at higher current density, it can be clearly seen that the TiO<sub>2</sub>/S composite have high capacity retention of 96%. While the capacity retention of pure S fades rapidly with the improvement of cycles. As for the reason of improvement of TiO<sub>2</sub>/S composite cathode, it is mainly attributed to the uniformly distribution of sulfur in the composite cathode materials [19]. This is beneficial for the enhancement of cycle stability of the cathode in the Li-S battery [20]. However, the pure S cathode suffers from severe capacity fading during the cycles, which is caused by the poor electronic conductivity and dissolution of polysulfide [21]. For the TiO<sub>2</sub>/S cathode, the metal oxide TiO<sub>2</sub> could deal with these problems at the same time.



**Figure 6.** (a) The comparison of cycle performance for TiO<sub>2</sub>/S and pure S at the current density of 0.5 C. (b) The capacity retention of two cathode materials at the current density of 0.5 C.

Rate performance is also an important index for judging the performance of the cathode materials. Based on this reason, a comparison of rate performance for the two cathode materials is made [22]. As shown in Figure 7, the specific capacity value of TiO<sub>2</sub>/S and pure S at various current densities from 0.1 C to 2 C is exhibited in the Figure. It can be clearly observed that the TiO<sub>2</sub>/S composite cathode displays perfect rate performance. Even at the high current density of 2 C, the capacity value of TiO<sub>2</sub>/S is 852 mAh g<sup>-1</sup>. Moreover, the capacity value recovers the pristine value when the current density comes back to 0.1 C. This improved rate performance is ascribed to the presence of hierarchically constructed TiO<sub>2</sub> spheres, which could inhibit the migration of polysulfide as an efficient polysulfide barrier. In all, the electrochemical performance of the Li-S batteries is greatly enhanced by using metal oxides TiO<sub>2</sub> as absorber for the polysulfide [23].



**Figure 7.** The comparison of rate performance for TiO<sub>2</sub>/S and pure S at various current densities from 0.1 C to 2 C.

To further confirm the excellent electrochemical performance of the as-prepared TiO<sub>2</sub>/S cathode materials, a table was made for the comparison between the TiO<sub>2</sub>/S and other reported cathode materials in the Li-S batteries. As shown in Table 1, it can be clearly seen that the TiO<sub>2</sub>/S cathode shows best electrochemical performance among various cathode materials. This is mainly due to the presence of metal oxide TiO<sub>2</sub> in the composites, which could enhance the electronic conductivity and inhibit the shuttle effect of polysulfide in the electrolyte. As a result, the cycle stability of the Li-S battery is greatly improved by using metal oxide TiO<sub>2</sub> as host materials for the element sulfur.

Therefore, this work may provide a promising method for preparing superior cathode material for Li-S batteries.

**Table 1.** The electrochemical performance of TiO<sub>2</sub>/S cathode compared with other cathode materials for the Li-S batteries.

Samples	Current Density	Capacity	Ref
C <sub>60</sub> nanorods	0.5 C	725 (100 cycles)	24
KB&MTO-GF	0.5 C	856 (100 cycles)	25
TiO <sub>2</sub> /S	0.5 C	968 (100 cycles)	This Work

#### 4. CONCLUSIONS

In summary, novel hierarchically constructed TiO<sub>2</sub> spheres are prepared and used host materials for sulfur cathode. This novel structure of TiO<sub>2</sub> spheres serves as the host material, which could efficiently stabilize the polysulfide at the cathode side. As a result, the TiO<sub>2</sub>/S composites exhibit excellent cycle stability and rate performance. The first specific capacity value is 1405 mAh g<sup>-1</sup> at the current density of 0.1 C. The capacity value is 968 mAh g<sup>-1</sup> at the current density of 0.5 C after 100 cycles. Even at the high current density of 2 C, the capacity value of TiO<sub>2</sub>/S is 852 mAh g<sup>-1</sup>.

#### ACKNOWLEDGEMENT

This work was supported by the Major National Science and Technology Projects (2017ZX04011010).

#### References

1. Y. P. Huang, X. G. Sun, J. Wang, X. Li, W. Chen, C. C. Wei, H. Hu and G. D. Liang, *J. Alloy Compd.*, 776 (2019) 187.
2. J. Ni, L. M. Jin, M. Z. Xue, J. S. Zheng, J. P. Zheng and C. M. Zhang, *Electrochim. Acta*, 296 (2019) 39.
3. Y. L. An, Y. Tian, H. F. Fei, G. F. Zeng, H. W. Duan, S. C. Zhang, P. Zhou, L. J. Ci and J. K. Feng, *Mater. Lett.*, 228 (2018) 175.
4. R. L. Yang, H. W. Du, Z. Q. Lin, L. L. Yang, H. Zhu, H. Zhang, Z. K. Tang and X. C. Gui, *Carbon*, 141 (2019) 258.
5. L. Y. Du, Q. Wu, L. J. Yang, X. Wang, R. C. Che, Z. Y. Lyu, W. Chen, X. Z. Wang and Z. Hu, *Nano Energy*, 57 (2019) 34.
6. X. H. Wang, Z. Wang, L. Z. Wang, Z. Q. Wang and H. Z. Guo, *J. Power Sources*, 414 (2019) 318.
7. Q. S. Wang, L. H. Jiang, Y. Yu and J. H. Sun, *Nano Energy*, 55 (2019) 93.
8. X. L. Lu, Q. F. Zhang, J. Wang, S. H. Chen, J. M. Ge, Z. M. Liu, L. L. Wang, H. B. Ding, D. C. Gong, H. G. Yang and B. G. Lu, *Chem. Eng. J.*, 358 (2019) 955.
9. Y. P. Huang, X. G. Sun, J. Wang, X. Li, W. Chen, C. C. Wei, H. Hu and G. D. Liang, *J. Alloy Compd.*, 776 (2019) 187.
10. R. H. Zhang, T. S. Zhao, H. R. Jiang, M. C. Wu and L. Zeng, *J. Power Sources*, 409 (2019) 76.
11. Y. Li, J. Chen, Y. F. Zhang, Z. Y. Yu, T. Z. Zhang and L. P. Zhang, *J. Alloy Compd.*, 766 (2018) 804.



12. Y. Q. Wang, S. Q. Luo, D. Q. Wang, X. B. Hong and S. K. Liu, *Electrochim. Acta*, 284 (2018) 400.
13. N. Li, X. He, K. H. Chen, S. Y. Chen and F. Y. Gan, *Mater. Lett.*, 228 (2018) 195.
14. N. Liu, L. Wang, Y. Zhao, T. Z. Tan and Y. G. Zhang, *J. Alloy Compd.*, 769 (2018) 678.
15. J. Wang, C. M. Fu, X. F. Wang, Y. M. Yao, M. L. Sun, L. N. Wang and T. X. Liu, *Electrochim. Acta*, 292 (2018) 568.
16. X. Y. Wen, K. X. Xiang, Y. R. Zhu, L. Xiao, X. H. Chen and H. Chen, *Mater. Lett.*, 229 (2018) 272.
17. P. H. Shao, J. Y. Tian, F. Yang, X. G. Duan, S. S. Gao, W. X. Shi, X. B. Luo, F. Y. Cui, S. L. Luo and S. B. Wang, *Adv. Funct. Mater.*, 28 (2018) 1705295.
18. Q. Sun, Y. Yang, Z. Zhao, Q. Zhang, X. Zhao, G. Nie, T. Jiao and Q. Peng, *Environ. Sci: Nano*, 5 (2018) 2440.
19. X. Y. Min, X. Wu, P. H. Shao, Z. Ren, L. Ding, X. B. Luo, *Chem. Eng. J.*, 358 (2019) 321.
20. N. Li, S. F. Tang, Y. D. Rao, J. B. Qi, Q. R. Zhang and D. L. Yuan, *Electrochim. Acta*, 298 (2019) 59.
21. H. Y. Yu, P. H. Shao, L. L. Fang, J. J. Pei, L. Ding, S. G. Pavlostathis and X. B. Luo, *Chem. Eng. J.*, 359 (2019) 176.
22. S. F. Tang, D. L. Yuan, Y. D. Rao, M. H. Li, G. M. Shi, J. M. Gu and T. H. Zhang. *J. Hazard. Mater.*, 366 (2019) 669.
23. R. Mezzenga, Q. R. Zhang, S. Bolisetty, Y. P. Cao, S. Handschin, J. Adamcik and Q. M. Peng, *Angew. Chem. Int. Edit.*, 2019, Doi: 10.1002/anie.201901596.
24. Y. L. An, Y. Tian, H. F. Fei, G. F. Zeng, H. W. Duan, S. C. Zhang and J. K. Feng, *Mater. Lett.*, 228 (2018) 175.
25. S. Lin, Y. R. Cai, J. Yang, F. X. Ruan, J. Wu, B. B. Sireesh, Y. Xin and J. M. Yao, *J. Alloy Compud.*, 779 (2019) 412.